"Reading" the photoelectron β-parameter spectrum in a resonance region

V. K. Dolmatov,[1,*] E. Guler,[1] and S. T. Manson[2,†]
[1]*Department of Physics and Earth Science, University of North Alabama, Florence, Alabama 35632, USA*
[2]*Department of Physics and Astronomy, Georgia State University, Atlanta, Georgia 30303, USA*
(Received 17 July 2007; published 6 September 2007)

The behavior of the dipole photoelectron angular distribution parameter $\beta_{nl}(\omega)$ in the vicinity of autoionizing resonances is discussed. It is shown that from this behavior, surprisingly, many photoionization parameters that cannot be measured experimentally can be extracted. These are the energy positions and ordering of autoionizing resonance minima in the partial photoionization cross sections σ_{l+1} and σ_{l-1}, the energies at which these two cross sections intersect, and signs and magnitudes of the $\cos(\delta_{l+1}-\delta_{l-1})$ ($\delta_{l\pm1}$ being the phase shifts of the dipole photoionization amplitudes $D_{l\pm1}$, respectively) through the autoionizing resonance energy region. Based on this, a deeper interpretation of such effects as the width-narrowing, width-fluctuating, and q-reversal in the β_{nl} parameter spectrum in the autoionizing resonance energy region is given. As an example, calculated data for partial photoionization cross sections $\sigma_{3d\rightarrow f}$ and $\sigma_{3d\rightarrow p}$, and β_{3d} parameters for $3d$ photoelectrons from Cr^+ are presented.

DOI: 10.1103/PhysRevA.76.032704 PACS number(s): 32.80.Dz, 32.80.Fb

I. INTRODUCTION

Spin-independent photoelectron angular distributions from gas-phase and condensed-phase matter—atoms, ions, molecules, clusters, solids, surfaces, etc.—are of considerable importance to both fundamental and applied sciences. The knowledge of these distributions provides, e.g., a way to map surface structure with regard to atomic positions on the surface [1]. Photoelectron angular distributions, in addition to the dependence on absolute values of partial photoionization amplitudes, depend on phase shifts of the photoionization amplitudes as well, thereby providing a stronger touchstone for testing various photoionization theories against experimental data. In addition, the combination of experimental data on these photoelectron angular distributions with both the data on angle-integrated photoionization cross sections and spin-dependent photoelectron angular distributions results in "complete" photoionization experiments [2]; the latter are aimed at extracting the information on otherwise nonobservable partial photoionization amplitudes and phase shifts from the experimental data. Thus, for many years now, there has been continuous interest in detailed studies of these distributions for a variety of species and regimes of photoionization, both in the dipole and, more recently, beyond the dipole approximations [3].

In the present paper, we focus on understanding the behavior of the dipole photoelectron angular distribution parameter β_{nl} in an autoionizing resonance energy region. Specifically, we focus on "reading" the β_{nl}-parameter spectrum in this region in the sense of extracting as much of "complete" information (dipole amplitudes and their relative phases) on the photoionization process as possible without the help of data on angle-integrated and spin-dependent photoionization parameters. We show, that, on many occasions, just by scrutinizing the resonance profile of the β_{nl} parameter in an autoionizing resonance region one can learn about (a) the energy positions and ordering of the autoionizing minima in partial (experimentally nonobservable) photoionization cross sections σ_{l+1} and σ_{l-1}, (b) where these cross sections are equal, i.e., where they intersect, and (c) the signs and approximate magnitudes of $\cos(\delta_{l+1}-\delta_{l-1})$ ($\delta_{l\pm1}$ being the phase shifts of the corresponding partial photoionization amplitudes) throughout the autoionizing resonance energy region. In essence, this is a continuation of our theory of complete experiments with fewer measurements [4]. Moreover, based on the results of the present work, natural explanations of the previously predicted [5,6] q-reversal, width-narrowing, and width-fluctuating effects in resonance structures in the β-parameter spectrum are given; these effects were uncovered calculationally, but their underlying interpretation has been lacking so far. The results of the present work are exemplified by corresponding calculations of the Cr^+ ion in the region of $3p\rightarrow 4s$ and giant $3p\rightarrow 3d$ resonances. The calculations were performed within the framework of the spin-polarized random phase approximation with exchange (SPRPAE) [7].

II. THEORETICAL BASIS

For 100% linearly polarized light, the differential photoionization cross section $d\sigma_{nl}/d\Omega$ of an nl-subshell within the dipole approximation is given by [8]

$$\frac{d\sigma_{nl}}{d\Omega}=\frac{\sigma_{nl}}{4\pi}\left(1+\frac{\beta_{nl}}{2}(3\cos^2\theta-1)\right). \tag{1}$$

Here, $\sigma_{nl}=\sigma_{l+1}+\sigma_{l-1}$ is the dipole photoionization cross section of an nl subshell, $\sigma_{l\pm1}$ are corresponding $nl\rightarrow\epsilon l\pm1$ partial photoionization cross sections, and β_{nl} is the dipole photoelectron angular asymmetry parameter [7],

$$\sigma_{l\pm1}=\frac{4\pi^2\alpha N_{nl}\hbar\omega}{3(2l+1)}(|D_{l\pm1}|^2), \tag{2}$$

*vkdolmatov@una.edu
†smanson@gsu.edu

$$\beta_{nl} = \frac{(l+2)|D_{l+1}|^2 + (l-1)|D_{l-1}|^2}{(2l+1)(|D_{l+1}|^2 + |D_{l-1}|^2)} + \frac{6\sqrt{l(l+1)}\mathrm{Re}(D_{l+1}D_{l-1}^*)}{(2l+1)(|D_{l+1}|^2 + |D_{l-1}|^2)}, \tag{3}$$

$$D_{l\pm1} = |D_{l\pm1}|\exp(i\delta_{l\pm1}). \tag{4}$$

Here, $\hbar\omega$ is the photon energy, α is the fine-structure constant, N_{nl} is the occupation number of the nl subshell, $\delta_{l\pm1}$ are the phases of the reduced photoionization amplitudes $D_{l\pm1}$ for the $nl \rightarrow l\pm1$ photoionization transitions, respectively. It is convenient to recast the expression for β_{nl} as [4]

$$\beta_{nl} = \frac{(l-1)\rho^2 + 6\sqrt{l(l+1)}\rho\cos\Delta + (l+2)}{(2l+1)(\rho^2+1)}, \tag{5}$$

where

$$\rho = \frac{|D_{l-1}|}{|D_{l+1}|}, \quad \Delta = \delta_{l+1} - \delta_{l-1}. \tag{6}$$

Note that the quantities $\sigma_{l\pm1}$, ρ, $\delta_{l\pm1}$, and Δ all depend upon photon energy; the explicit dependence is omitted in the above equations for reasons of simplicity.

Concerning extrema in β_{nl} due to an autoionizing resonance excitation, to a good approximation, when $\cos\Delta(\omega)$ is effectively constant around the extrema, they occur at [4]

$$\rho = -\frac{1}{2\sqrt{l(l+1)}\cos\Delta} + \sqrt{\frac{1}{4l(l+1)\cos^2\Delta} + 1}, \tag{7}$$

which translates to

$$\beta_{nl}^{\max/\min} = (2l+1)^{-1}\left(l - 1 \pm \frac{6l(l+1)\cos^2\Delta}{\sqrt{1 + 4l(l+1)\cos^2\Delta} \mp 1}\right), \tag{8}$$

for $\cos\Delta$ positive and negative, respectively; the former representing a maximum in β_{nl}, and the latter a minimum. This opens the road for complete experiments with fewer measurements [4], where one can "measure" $D_{l\pm1}$ and $\cos\Delta$ at the β_{nl}'s extreme points without performing complicated spin-polarized measurements. It is shown below that, actually, $\cos\Delta$ can be specified not only at the extreme points but through the entire resonance energy region as well. Note, the sign of $\cos\Delta$ changes by π at photon energies corresponding to autoionizing resonance *minima* in either of the two partial cross sections $\sigma_{l\pm1}$. Indeed, the autoionizing minima in $\sigma_{l\pm1}$ occur where the real and imaginary parts of a photoionization amplitude $D_{l\pm1}$ pass a zero, thereby changing their signs. Then, in accordance with Eq. (4), the amplitude's phase shift $\delta_{l\pm1}$ changes by π, so Δ changes by π as well, causing the $\cos\Delta$ term to change its sign.

To proceed, we make two reasonable assumptions. First, generally, one of $D_{l\pm1}$ amplitudes far dominates over the other in the autoionizing resonance energy region except where they have autoionizing resonance minima (since the latter are located at different photon energies). We thus assume that, as normally happens, the $l+1$ transition is the dominant transition. Second, we assume that

$$\frac{1}{2\sqrt{l(l+1)}\cos\Delta} \ll 1. \tag{9}$$

In fact, Eq. (9) is already satisfied when

$$|\cos\Delta| \gg \begin{cases} 0.3 & \text{for } l=1, \\ 0.2 & \text{for } l=2, \\ 0.1 & \text{for } l=3. \end{cases} \tag{10}$$

Looking at these numbers, it is very suggestive that Eq. (9) could, actually, be a rather general occurrence for autoionizing resonances well above threshold in nl photoionization of atoms, especially for $l \geq 2$. The closer $\cos\Delta$ is to unity, the more precise are the predictions.

It readily follows then, that the $\beta_{nl}(\omega)$ parameter maximizes or minimizes at energies $\omega_{\max}$ and $\omega_{\min}$, respectively, where $\rho \approx 1$, i.e., when $|D_{l+1}| \approx |D_{l-1}|$ (or $\sigma_{l-1} \approx \sigma_{l+1}$). This can happen only within a region of the autoionizing resonance minimum (zero) in the normally dominant partial cross section σ_{l+1} where the latter yields to σ_{l-1}. Hence, the key to the understanding of details of autoionizing resonance spikes in the β-parameter spectrum lies in the interplay of autoionizing *minima* in σ_{l+1} and σ_{l-1} such as the relative positions of the minima, their shapes, and the details of where and how σ_{l+1} and σ_{l-1} intersect ($\rho=1$) in the energy domain under scrutiny. Whatever happens to the $\sigma_{l\pm1}$ in the region of their autoionizing resonance *maxima* is irrelevant for the resonance behavior of the β_{nl} parameter. An important consequence of this is that the widths, strengths, shapes, and positions of the autoionizing resonance spikes in $\beta_{nl}(\omega)$ have little to do with those for the autoionizing resonance *maxima* in related angle-integrated cross sections $\sigma_{l\pm1}$.

To summarize the collection of the most important issues needed for "reading" the β_{nl}-parameter spectrum within the developing methodology in this paper, we require Eq. (8) plus

$$\beta_{nl} = \beta_{nl}^{\max/\min} \quad \text{at } \rho \approx 1 (\sigma_{l+1} \approx \sigma_{l-1}), \tag{11a}$$

$$\cos\Delta \approx \text{const} \quad \text{around } \beta_{nl} = \beta_{nl}^{\max/\min}, \tag{11b}$$

$$\beta_{nl} = \frac{l-1}{2l+1} \quad \text{at } \sigma_{l+1} \ll \sigma_{l-1} \ (\rho \gg 1), \tag{11c}$$

$$\beta_{nl} = \frac{l+2}{2l+1} \quad \text{at } \sigma_{l+1} \gg \sigma_{l-1} \ (\rho \ll 1), \tag{11d}$$

$$\delta_{l\pm1} \rightarrow \delta_{l\pm1} + \pi \quad \text{at } \sigma_{l\pm1} = 0, \tag{11e}$$

$$\cos\Delta \rightarrow -\cos\Delta \quad \text{at } \sigma_{l\pm1} = 0. \tag{11f}$$

Equations (11c) and (11d) were not discussed above, but they readily follow from Eq. (5). It is shown in the next section that Eqs. (11a)–(11f) and Eq. (8) allow us to extract information (from the β_{nl}-parameter spectrum) on (a) the magnitudes and signs of $\cos\Delta$ through the autoionizing resonance region, and (b) the positions of autoionizing resonance minima (zeros) in σ_{l+1} and σ_{l-1}, and where these cross sections intersect.

III. RESULTS AND DISCUSSION

A. $3p \rightarrow 4s\ ^6P_{3/2,5/2,7/2}$ resonances in β_{3d} for $Cr^+(3p^6d^5\ ^6S)$

The $3d$ photoelectron angular distribution from the $Cr^+(3p^63d^5\ ^6S)$ ion in the region of the $3p^63d^5$, $^6S \rightarrow 3p^53d^54s$, $^6P_{3/2,5/2,7/2}$ and $3p^63d^5$, $^6S \rightarrow 3p^53d^6$, $^6P_{3/2,5/2,7/2}$ autoionizing resonances (termed $3p \rightarrow 4s$ and $3p \rightarrow 3d$ resonances, respectively), decaying into $3p^63d^4\epsilon f, p$ $(3d \rightarrow \epsilon f, 3d \rightarrow \epsilon p)$ continuum, provides a good illustrative case study. First, not only will it allow us to exhibit the predictive nature of the methodology developed, but it also sheds light on physics behind the width-narrowing and q-reversal effects predicted earlier, but not well-understood, in the Cr^+ β_{3d}-parameter spectrum [6]. Second, the weak $3p \rightarrow 4s\ ^6P_{3/2,5/2,7/2}$ resonances in Cr^+, whose energies [9–11] are E_r=41.68, 41.39, and 41.02 eV, respectively, are in close proximity to a $3p \rightarrow 3d$ giant resonance ($E_r \approx 44.29$ eV [9–11], a profile index $q \approx 2.9$, and half-width $\Gamma \approx 1.2$ eV [11]), and the corresponding SPRPAE calculations of the Cr^+ $3d$ photoionization cross section σ_{3d} within these interacting $3p \rightarrow 4s\ ^6P_{3/2,5/2,7/2}$ and $3p \rightarrow 3d$ resonances [12] are in reasonable agreement with the experimental data [10,11]. Therefore, it is expected that SPRPAE is also reasonably accurate for the Cr^+ $3d$ photoelectron angular distribution as well.

Calculated SPRPAE results for the Cr^+'s β_{3d} [6], as well for $\cos\Delta$, and $\sigma_{l\pm1}$ within the region of the $3p \rightarrow 4s\ ^6P_{7/2,5/2,3/2}$ resonances are shown in Fig. 1. The SPRPAE calculations were performed exactly in the same manner as described earlier elsewhere [6,12] for which reason we omit their discussion in this paper; we focus on illustration only as how to extract "complete" information from the β-parameter spectrum rather than to make the most precise calculations possible.

As an example, we "read" the β_{3d} ($^6P_{7/2}$) multiplet component (upper panel in Fig. 1) to extract information about $\sigma_{l\pm1}$, and $\cos\Delta$ within the energy region in question.

First, we find that the maximum and minimum in β_{3d}, $^6P_{7/2}$ are located at ω_{max}=40.28 eV and ω_{min}=40.38 eV, respectively. Correspondingly, this predicts that these are energies, where $\rho \approx 1$, i.e., where $\sigma_{l+1}(\omega)$ and $\sigma_{l-1}(\omega)$ intersect, $\sigma_{l+1}=\sigma_{l-1}$. Looking at $\sigma_{l+1}(\omega)$ and $\sigma_{l-1}(\omega)$ calculated directly, it is found that they intersect at ω_1^{calc}=40.29 eV and ω_2^{calc}=40.41 eV; these are in excellent agreement with the predicted intersection energies.

Second, from Eq. (11c) for l=2, β_{3d}=0.2 at $\omega \equiv \omega_+$ where σ_{l+1}=0, whereas β_{3d}=0.8 at $\omega \equiv \omega_-$ where σ_{l-1}=0. From the calculated β_{3d} for the $^6P_{7/2}$ channel, we then predict, that σ_{l+1}=0 at $\omega_+ \approx 40.33$ eV, which agrees exactly with the direct calculation. Looking at where β_{3d}=0.8, we predict that σ_{l-1} could be zero either at $\omega_-^{(1)} \approx 40.18$ eV, or $\omega_-^{(2)} \approx 40.31$ eV. The solution $\omega_-^{(2)} \approx 40.31$ eV must be discarded as extraneous; otherwise it is not possible to satisfy the condition that $\sigma_{l-1} > \sigma_{l+1}$ *only* between ω_{max}=40.28 eV and ω_{min}=40.38 eV intersection points, where β_{3d} is maximized and minimized, respectively. Thus, we predict that σ_{l-1}=0 at $\omega_- \approx 40.18$ eV, in excellent agreement with the calculated energy of 40.19 eV. In the same manner, it can easily be understood that the relative ordering of the maximum and minimum in β_{nl} is related to the relative ordering of minima in σ_{l+1} and σ_{l-1}. Specifically, if the minimum of β_{nl} is preceded by its maximum (as, e.g., in the upper panel in Fig. 1), then the minimum in σ_{l+1} must be preceded by the minimum in σ_{l-1}if $\cos\Delta$ is negative, and vice versa.

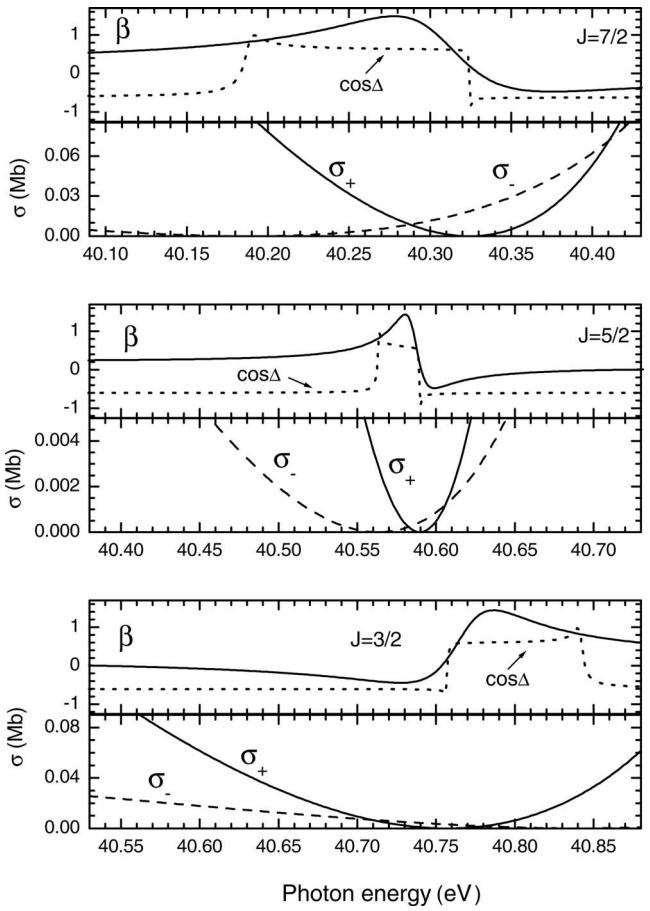

FIG. 1. Calculated SPRPAE results for the $3d$ photoelectron angular distribution parameter $\beta_{3d}(\omega)$, partial photoionization cross sections $\sigma_\pm \equiv \sigma_{l\pm1}$ (Mb), and $\cos\Delta$ in the region of the multiplet split resonance components $3p \rightarrow 4s\ ^6P_{3/2,5/2,7/2}$ in the Cr^+ ion.

Now that the positions of minima in the $\sigma_{l\pm1}$ have been found, one can predict signs and magnitudes of $\cos\Delta(\omega)$ in this energy region. Since $\beta_{3d}^{max} \approx 1.5$ and is maximized when $\cos\Delta > 0$, we predict, from Eq. (8), that $\cos\Delta \approx +0.6$ at ω_{max}=40.28 eV. This is in good agreement with the calculated data. Then, consider going from this energy, ω_{max}=40.28 eV, towards higher energies. At the energy $\omega_+ \approx 40.33$ eV, where σ_{l+1}=0, the photoionization amplitude D_{l+1} changes sign. Hence, at $\omega \approx 40.33$ eV, according to Eq. (11e), the phase shift δ_{l+1} changes suddenly by π. Correspondingly, from Eq. (11f), we predict, that $\cos\Delta$ will change suddenly from positive, $\cos\Delta \approx 0.6$, to negative, $\cos\Delta \approx -0.6$, at $\omega \approx 40.33$ eV, and it will retain this value towards higher energies, including the energy at which β_{3d} is a minimum. This is in good agreement with the calculated data as well. Next, moving from the original energy ω_{max}=40.28 eV, where β_{3d} is maximized, towards lower energies, we predict, that $\cos\Delta \approx +0.6$ until $\omega=\omega_- \approx 40.18$ eV, where σ_{l-1}=0, i.e., where D_{l-1} changes

its phase by π. At this energy $\cos\Delta$ will suddenly change to negative, $\cos\Delta \approx -0.6$, and retain this value at lower energies. This is what is indeed seen from the calculated results for $\cos\Delta$.

To summarize, looking at the autoionizing resonance profile of the β_{nl} parameter, one can "read" quite a bit of information concerning partial photoionization cross sections and phase shifts of photoionization amplitudes, i.e., on quantum mechanical quantities that cannot be observed directly experimentally.

B. Width-narrowing, width-fluctuating, and *q*-reversal effects in Cr^+ $\beta_{nl}(\omega)$

One can now interpret the width-narrowing, width-fluctuating, and *q*-reversal (symmetry-reversal) phenomena in the β-parameter spectrum, predicted theoretically some years ago [5,6], but not really well-understood even now.

Consider these phenomena in the same case study, the $3p \rightarrow 4s\ ^6P_{7/2,5/2,3/2}$ resonances in $3d$ photoionization of Cr^+, seen in Fig. 1. The phenomena listed above result in the profile of the $3p \rightarrow 4s\ ^6P_J$ resonance variation in a J-resolved β_{3d}^J either getting much narrower (the width-narrowing effect; compare the $J=5/2$ results with the two other J's in Fig. 1) or changing its symmetry (*q*-reversal effect; compare the $J=3/2$ result with the two others in the same figure) as a function of the energy distance of the given J component from the nearby $3p \rightarrow 3d$ giant resonance (not displayed in Fig. 1) [6]. One can also note the width-fluctuating effect [5] in the case study which results in the width of the resonances in β_{nl}^J first narrowing and then broadening again (or vice versa) as a function of J.

Having shown above that autoionizing resonance minima and maxima in β_{nl} occur at energies where $\rho \approx 1$, i.e., where σ_{l-1} and σ_{l+1} intersect, it is easy to understand the width-narrowing (width-broadening) effect. It is simply a reflection of that fact that the minima in σ_{l+1} and σ_{l-1} are getting closer to or farther from each other and/or the minimum in the dominant cross section becomes deeper or shallower. When this happens, the energy distance between the two points of intersection between σ_{l+1} and σ_{l-1} gets smaller or larger, thus resulting in the narrower or broader width of a resonance spike in β_{nl}. Indeed, this interpretation is in agreement with the calculated results displayed in Fig. 1.

As for the *q*-reversal effect, i.e., when the positions of the maximum and minimum in β_{nl} swap, it reflects the change in a relative ordering of autoionizing resonance minima in σ_{l-1} and σ_{l+1} to the opposite ordering. This is why the β_{3d} $J=3/2$ spectrum in Cr^+ exhibits symmetry opposite to the $J=7/2$ and $J=5/2$ spectra.

The reason why all three effects—the width-narrowing, the *q*-reversal, and the width-fluctuating effects—are seen in β_{3d} of Cr^+ is that the related multiplet resonance components $3p \rightarrow 4s\ ^6P_{7/2,5/2,3/2}$ are in close proximity to the $3p \rightarrow 3d$ giant resonance [6,10]. Therefore, small differences in positions of each of $3p \rightarrow 4s\ ^6P_{7/2,5/2,3/2}$ resonances relative to the $3p \rightarrow 3d$ giant resonance alter the autoionizing minima in the $\sigma_{l\pm1}$ where these cross sections are the smallest, strongly and *differently*. This, in turn, is reflected in noticeable changes in multiplet resonance spikes in β_{3d}, bringing in all three of these effects in evidence in one β_{nl}-parameter spectrum.

IV. CONCLUSION

In conclusion, we have shown that autoionizing resonance variations in the β_{nl}-parameter spectrum are critically related to shapes and relative positions of autoionizing resonance minima in the partial photoionization cross sections σ_{l+1} and σ_{l-1}, and to where these cross sections intersect. Correspondingly, all this information can be "read" from the β_{nl}-parameter spectrum. In addition, the signs and magnitudes of $\cos\Delta$ through the whole resonance region can be extracted from the β_{nl}-parameter spectrum as well, without the need to resort to complicated spin-polarized measurements. Moreover, using the methodology introduced in this paper, we have provided a simple interpretation of the previously predicted width-narrowing, width-fluctuating, and q-reversal effects in the β_{nl}-parameter spectrum in the autoionizing resonance energy region.

Note, that in energy region where $\cos\Delta$ varies rapidly as a function of ω, such as near threshold owing to a shape resonance or the rapid variation of Coulomb phase shift, this analysis will not apply [4]. Also, when conditions listed in Eq. (10) are not met, the predictions of energies at which β_{nl} is maximized or minimized will be less precise than when $\cos\Delta$ is of the order of unity as assumed in this paper. These conditions which obviate the "reading" of the β_{nl}-parameter spectrum will occur mostly at near threshold energy. But away from threshold the theory should generally be applicable. Furthermore, when resonances are not isolated but strongly exist as interacting resonances, or when there are more than two channels for the photoionization process, the analysis presented here might need to be generalized. Nevertheless, the ideas presented in the paper might be useful as the first step in attempting to "read" the β_{nl}-parameter spectrum even for such situations.

ACKNOWLEDGMENTS

This work was supported by NSF Grants Nos. PHY-0652704 and PHY-024394, and DOE, Division of Chemical Sciences, BES Grant No. DE-FG02-03ER15428.

[1] C. J. Fisher, R. Ithin, R. G. Jones, G. J. Jackson, D. P. Woodruff, and B. C. C. Cowiex, J. Phys.: Condens. Matter **10**, L623 (1998).
[2] N. A. Cherepkov and S. K. Semenov, J. Phys. B **37**, 1267 (2004).
[3] O. Hemmers, R. Guillemin, and D. W. Lindle, Radiat. Phys. Chem. **70**, 123 (2004).
[4] V. K. Dolmatov and S. T. Manson, Phys. Rev. A **58**, R2635

(1998).
[5] J.-P. Connerade and V. K. Dolmatov, J. Phys. B **30**, L181 (1997).
[6] V. K. Dolmatov and S. T. Manson, J. Phys. B **30**, L517 (1997).
[7] M. Ya. Amusia and L. V. Chernysheva, *Computation of Atomic Processes* (IOP, Bristol, 1997).
[8] S. T. Manson and A. F. Starace, Rev. Mod. Phys. **54**, 389 (1982).
[9] J. T. Costello, E. T. Kennedy, B. F. Sonntag, and C. W. Clark, Phys. Rev. A **43**, 1441 (1991).
[10] C. McGuinness, M. Martins, Ph. Wernetk, B. F. Sonntag, P. van Kampen, J.-P. Mosnier, E. T. Kennedy, and J. T. Costello, J. Phys. B **32**, L583 (1999).
[11] J. B. West, J. E. Hansen, B. Kristensen, F. Folkmann, and H. Kjeldsen, J. Phys. B **36**, L327 (2003).
[12] V. K. Dolmatov, J. Phys. B **29**, L673 (1996).